DUJASE Vol. 7 (1) 9-15, 2022 (January) https://doi.org/10.3329/dujase.v7i1.62881

Study of the Perturbation in Temperature Profile of an AGR Fuel Pin for Surface Roughness of Cladding by CFD Simulation in Ansys Fluent

Sadek Hossain Nishat, Farhana Islam Farha and Md. Hossain Sahadath*

Department of Nuclear Engineering, University of Dhaka, Dhaka-1000

**E-mail:hossain_ne@du.ac.bd*

Received on 10 June 2021, Accepted for publication on 15 October 2021

ABSTRACT

The surface roughness of nuclear fuel cladding plays a crucial role in the thermal-hydraulic response of the Advanced Gas Cooled reactor (AGR). In the present work, the change in the temperature distribution from an isolated AGR fuel rod to primary coolant due to cladding roughness was studied by computational fluid dynamics (CFD) simulation in Ansys Fluent software. Square transverse ribs of the various pitch to height ratios (p/k) were considered as the surface roughness. Radial temperature profiles from fuel to coolant were generated. Lower fuel temperature was found for the fuel rod with a rough cladding surface as compared to the smooth cladding surface. The peak fuel temperature was determined and found to decrease with decreasing values of (p/k). Temperature drop across the fuel and from fuel to coolant was also studied.

Keywords: AGR, CFD, Fluent, Fuel Rod, Ribs, Temperature.

1. Introduction

The well-defined single phase of the gaseous coolant ensures the enhanced safety of the gas-cooled nuclear reactor even in emergency conditions. Unlike liquid coolants, it remains in the gaseous phase if the reactor core temperature increases due to undercooling of the nuclear fuel elements. Moreover, a much higher core exit temperature of the gaseous coolant allows producing superheated steam in the secondary circuit which is used as the working fluid of the turbine. This higher temperature steam results in a higher plant thermal efficiency ($\geq 40\%$) as compared to the conventional light water reactor ($\sim 33 - 34\%$) [1]. However, the thermal conductivity and heat transfer coefficient of gaseous coolant is much lower than that of the liquid coolants (e.g. water). The comparatively lower values of these parameters demand the necessity of the heat transfer enhancement process. Basically, there are two types of heat transfer augmentation techniques. In the passive techniques, surface modification is used to change the existing flow mechanism and heat transfer improvement occurs due to an increase in the flow friction and pressure drop. The active augmentation technique uses an external power to get the desired flow modification. The heat transfer surface vibration, fluid vibration, and electric field introduction are some of the examples of this category [2].

The Advanced Gas Cooled Reactor (AGR) is a nuclear reactor design used in the United Kingdom. Gaseous carbon dioxide is used as a primary coolant which is heated by the energy released from nuclear fission in the fuel rods. Since the primary coolant (CO_2) is in the gaseous phase, therefore the heat transfer rate from fuel to the coolant is comparatively lower than LWR. The higher flow rate can be utilized to enhance heat transfer but it requires higher pumping power. On the other hand, an increase in coolant channel volume increases core size that changes the core neutronic design parameters [3]. The most popular and successful technique is augmentation through surface roughness. The higher surface area of the rough surface contributes to the heat transfer augmentation process. This enhanced heat transfer from the fuel rod to reactor coolant (CO_2) changes the radial temperature distribution of the fuel pin. Several works [4-8] are found in the literature regarding the heat transfer augmentation of AGR fuel and rough heated surfaces. Little works are found on the effect of cladding surface roughness on the fuel temperature distribution for different pitch-to-height ratios of square transverse ribs. The purpose of the present study is to determine the perturbation in the fuel temperature profile of an isolated fuel rod of AGR with a rough cladding surface. The computational fluid dynamics (CFD) code Ansys Fluent was used to perform the simulation. The square transverse ribs (helix angle is 90°) of the various pitch-to-height ratio (6-12) were considered as surface roughness. Each of the cases has been compared with the values for the fuel rod with a smooth cladding surface. The maximum fuel temperature and the temperature drop within the fuel and from fuel centerline to coolant region were also studied.

2. Materials and Method

2.1 Geometry of the work

The simulation was carried out for an isolated fuel rod with its surrounding coolant region. The three different domains of the geometry include a central solid fuel region followed by a solid cladding which is surrounded by a fluid domain. This fluid domain represents the coolant region. Figure 1 represents the cross-sectional view of the geometry. The specification of an AGR and the dimension of the geometry are given in Table 1. The square and transverse type ribs ($\alpha = 90^{\circ}$) are used as the surface roughness of the cladding. The pitch-to-height ratio of the ribs was taken from 6 to 12. Figure 2 shows the smooth and rib-roughed cladding surfaces considered in this study.

Table 1: Design Specification of AGR [9]

Thermal output	1623 MW_t
Moderator	Graphite
Coolant gas	CO_2
Mean gas pressure	44 bar
Mean inlet temperature	339 °C
Mean outlet temperature	639 °C
Average channel flow	12 kg/s
Fuel	UO_2
Enrichment	2.2-2.7 %
Pellet diameter	14.5 mm
Fuel length	900 mm
Rod pitch	25.7 mm
Cladding material	Stainless steel
Cladding thickness	0.38 mm
Assembly Type	36 pin cluster
Inner graphite sleeve diameter	190 mm
Channel diameter	264 mm
Guide tube diameter	16.27 mm
Power density	3 kW/liter
Linear heat generation rate	17 kW/m

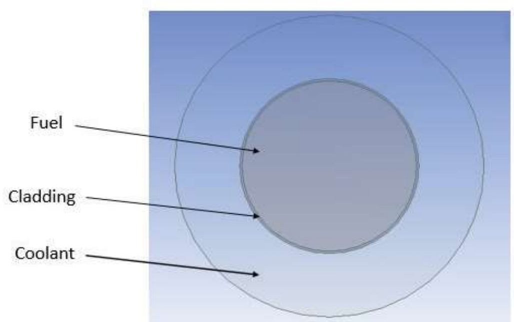

Fig. 1. AGR fuel pin with its neighborhood coolant region

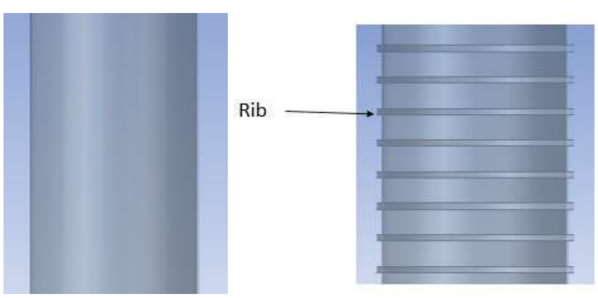

(a) (b)

Fig. 2. Fuel rod(a) smooth cladding surface, (b) rib-roughed cladding surface

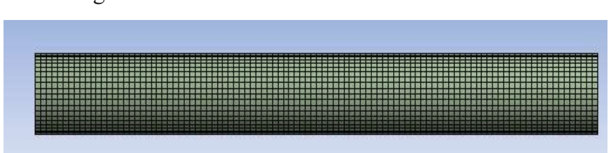

Fig. 3. Mesh of the geometry

2.2 Properties of Fuel, Cladding, and Coolant Materials

The chemical composition of the nuclear fuel of AGR is ceramic uranium dioxide (UO_2). Several properties viz. physical density, specific heat, and most importantly thermal conductivity of UO_2 are needed to perform the simulation in Fluent. Table 2 shows the average values of these parameters for the range of $1000°C$ to $1500°C$. These values were used in the present study as the fuel temperature of AGR covers this range. The cladding of the fuel is SS-2025 which is stainless steel. The surface roughness was introduced on it. The same physical properties are required as for the fuel and these are also temperature-dependent. Table 2 contains the average values of these parameters for the typical cladding temperature range of 1000℃ to 800℃ .The physical properties of the coolant CO_2 are both temperature and pressure-dependent. The values were taken at the average of the inlet and outlet temperature (489℃) and average coolant pressure (4.4MPa) and given in Table 2.

Table 2: Average values of physical properties for 1000℃ to 1500℃

Property (unit)	Fuel (UO_2) [10]	Cladding SS-2025 [11]	Coolant (CO_2) [12]
Density (kg/m^3)	10530	7950	30.012
Specific Heat $\left(\text{Jkg}^{-1}\text{k}^{-1}\right)$	328.775	571.4	1212
Thermal Conductivity $\left(\text{Wm}^{-1}\text{k}^{-1}\right)$	3.0	24.53	0.054
Dynamic Viscosity ($\text{kgm}^{-1}s^{-1}$)	----	----	3.383×10^{-5}

Nomenclature

A	Cross-sectional area of the flow channel
C_p	Specific heat
d	Diameter of fuel pellet
d_h	Hydraulic diameter, $4A/P_T$
d_i	Inner diameter (coolant region)
d_o	Outer diameter (coolant region)
d_G	Diameter of guide tube
d_R	Diameter of fuel rod
d_S	Diameter of inner graphite sleeve
h	Convective heat transfer coefficient

I	Turbulent intensity
´ k	Thermal conductivity
k	Height of rib
l	Length of fuel rod
L_C	Characteristic length
p	Pitch between two ribs
P_{ave}	Average coolant pressure
P_T	Total wetted perimeter
q'	Average linear heat generation rate
q'''	Volumetric heat generation rate,
Re	Reynolds number
T_m	Mean coolant temperature
u_m	Mean coolant velocity
□	Dynamic viscosity
A	Physical density
±	Helix angle of rib

2.3 Methodology

The modeled cases were solved using Ansys Fluent software, version 17.2. The simulation was carried out for each of the p/k values using the required input parameters and boundary conditions. For comparison, an AGR fuel rod with a smooth cladding surface was also simulated in the same condition. Since the study is performed by a numerical procedure using CFD simulation, it requires meshing of the geometry. The minimum mesh element size is $3.025\times10^{-2}\text{mm}$ while the maximum value is 2mm and a growth rate of 1.20 is considered. The standard k-ε turbulence model in ANSYS Fluent was used [13]. Boundary layer approximation is required for the turbulent flow analysis and for this reason inflation layers were adopted to the study geometry. These layers are given in the coolant part at the inner side of the annular coolant region. The calculated first layer height of these layers is 0.04889mm. The multizone mesh method was used to adjust structural mesh in the coolant domain to the meshing of the solid domain.

2.3.1 Boundary Conditions

The required input parameters for simulation in the Ansys Fluent include the average volumetric heat generation rate of nuclear fuel (q'''), mean coolant velocity (u_m), average coolant pressure (P_{ave}), mean coolant temperature (T_m), Reynolds Number (Re), and the turbulent intensity (I). In this study, T_m was considered 489 $°\text{C}$, P_{ave} of 4.4 MPa was taken from Table 1. Rests of the parameters are determined by analytical calculation using the design data of Table 1. The volumetric heat generation rate of AGR fuel is found using the following equation,

$$q''' = \frac{q'\times l}{(\text{À}/4)\times d^2\times l}\ldots\ldots\ldots\ldots\ldots(1)$$

The coolant flow area of a fuel channel was calculated from eq.(2),

$$A = (\text{À}/4)\left[d_S^2 - 36d_R^2 - d_G^2\right]\ldots\ldots\ldots.(2)$$

The average channel flow rate can be written as

$$\dot{m} = \text{Á}\times A\times u_m\ldots\ldots\ldots\ldots\ldots(3)$$

The eq. (3) was rearranged to calculate the mean coolant velocity from eq. (4)

$$u_m = \frac{\text{Á}\times A}{\dot{m}}\ldots\ldots\ldots\ldots\ldots\ldots\ldots.(4)$$

The hydraulic diameter was calculated by eq. (5) for calculating the Reynolds number (Re). The hydraulic diameter (d_h) for the annular coolant geometry of the study is written as,

$$d_h = \frac{4\times\left\{(\text{À}/4)\times d_o{}^2 - (\text{À}/4)\times d_i{}^2\right\}}{(\pi d_o + \pi d_i)}\ldots.(5)$$

After simplification,

$$d_h = d_o - d_i\ldots\ldots(6)$$

Putting the values of d_i (14.88mm) and d_0 (25.7mm) into this equation, the hydraulic diameter of this study was found 10.82mm. Reynolds Number was calculated eq. (6) considering $L_C = d_h$

$$\text{Re} = \frac{\rho u_m L_C}{\mu}\ldots\ldots\ldots\ldots\ldots\ldots(7)$$

The turbulent intensity (I) was calculated from the following equation.

$$I = 0.16\text{Re}^{(-1/8)}\times100\%\ldots\ldots\ldots\ldots(8)$$

A summary of calculated parameters alongside their contribution as a boundary condition in Ansys Fluent is given in Table 3.

Table 3: Calculated input parameters

Parameter	Calculated Value	Contribution as Boundary conditions (BC)
q'''	$102.95 MW/m^3$	Source term of fuel zone
u_m	$18 ms^{-1}$	BC of the coolant inlet
P_{ave}	$4.4 MPa$	BC of coolant outlet
T_m	489	BC of both inlet and outlet side
Re	172780	Not BC, used to calculate I
I	3.54%	BC of both inlet and outlet side
d_h	10.82mm	BC of both inlet and outlet side

2.3.2 Verification of Ansys Fluent

Before starting the simulation for the geometry of the present work, it is necessary to verify the installation and working environment of the Ansys Fluent. To validate the software, a reference model is taken from the literature [14]. The objective of the study was to enhance the turbulent heat transfer using Ag/HEG nanofluid with water. The geometry or specimen of the reference model is a simple circular pipe with diameter, $D = 0.01m$, and length, $L = 0.8m$. The model was simulated in the same condition in Fluent and the results were compared with the literature value. A good agreement between the results ensured the proper functioning of the software.

Table 4: Comparison between results of literature and present simulation

Nanofluid (Vol %)	Convective heat transfer coefficient $(Wm^{-2}k^{-1})$		
	Literature value	Present simulation	Error(%)
0.1	8331.330	8360.878	0.34
0.2	8325.994	8355.550	0.36
0.3	8318.003	8346.916	0.35
0.5	8297.430	8332.325	0.42
0.7	8278.277	8317.550	0.47
0.9	8259.868	8297.233	0.45

3. Results and Discussion

The energy released from nuclear fission appears as the kinetic energy of fission products, free neutrons, prompt and delayed gamma-ray, and beta particles. The kinetic energy of the fission products constitutes about 85% of the total fission energy. Due to the short range of the fission product, these energies are deposited around the fission site within the fuel. The energy of the rest of the particles mentioned above is deposited in the fuel, moderator, and structural materials of the core. On average, approximately 90% of the fission energy is deposited in the fuel rod, and the remaining 10% of energy deposition is distributed in materials other than fuel [3]. The biggest advantage of nuclear energy is the high specific power (power per unit fuel mass) of nuclear fuel e.g. uranium. This results in a high temperature of nuclear fuel rod which contains fissionable materials. The generated heat is transported first across the solid fuel pellets via thermal conduction and then across the gas gap separating the fuel pellets from the cladding to avoid pellet cladding interaction. The next step is the conduction through the cladding and finally, heat is transferred from the fuel cladding surface to the coolant by forced convection. There are certain design limitations on the allowable fuel temperature. The fuel centerline temperature is limited by the melting point of the fuel. Hence, there is a constraint on the temperature drop from fuel to coolant which in turn imposes a limitation on core linear power density [15]. However, linear power density must be increased to minimize the size of the reactor core. To accomplish this, there is a motivation to increase the heat transfer from fuel to the coolant by increasing the thermal conductivity of fuel and cladding and convective heat transfer coefficient of the coolant. One of the successful techniques to increase the convective heat transfer coefficient is to increase the surface area of the heated surface. In a nuclear reactor like AGR, the heated surface is the fuel rod cladding surface. On the other hand, the thermal conductivity of nuclear fuel (UO_2) decreases with temperature (550-2000K) at the operating condition of the reactor [16-18]. Therefore, lower fuel temperature results in a higher thermal conductivity and higher heat transfer. This can be achieved by augmentation techniques like surface roughness.

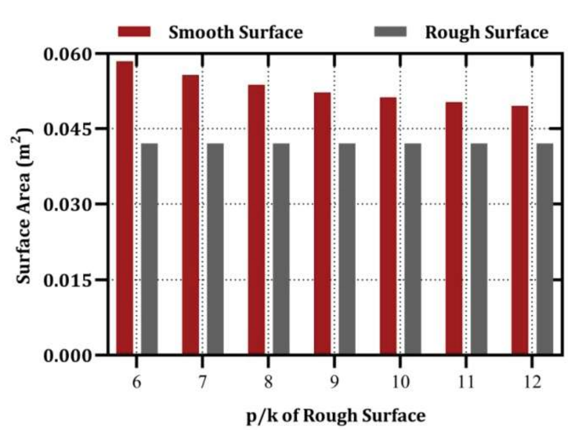

Fig. 4. Comparison of fuel cladding surface area

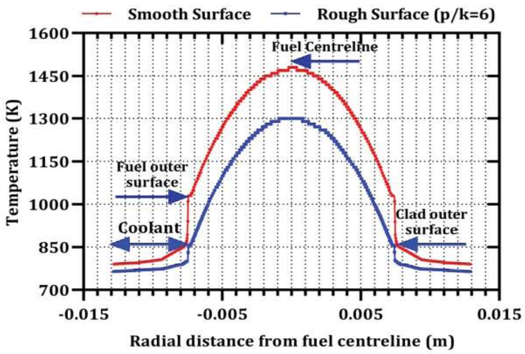

(a)

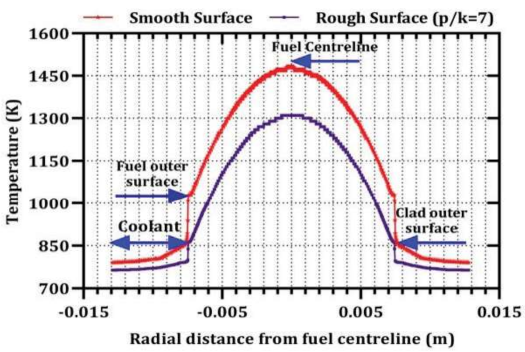

(b)

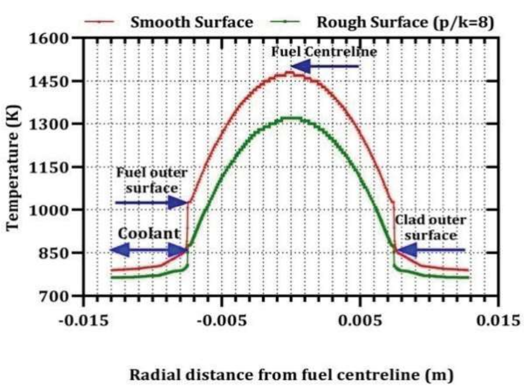

(c)

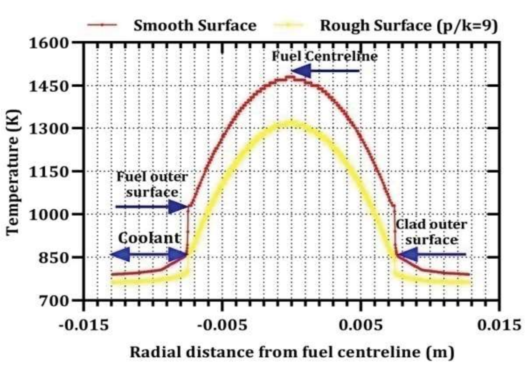

(d)

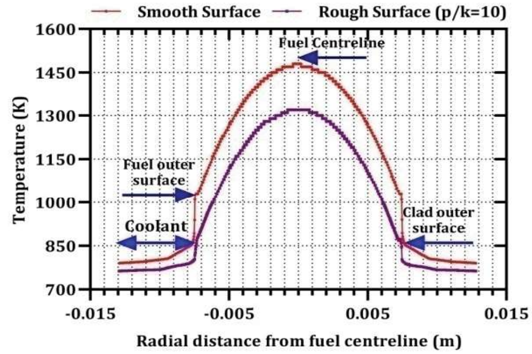

(e)

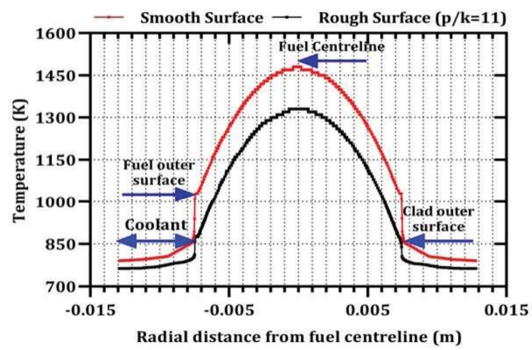

(f)

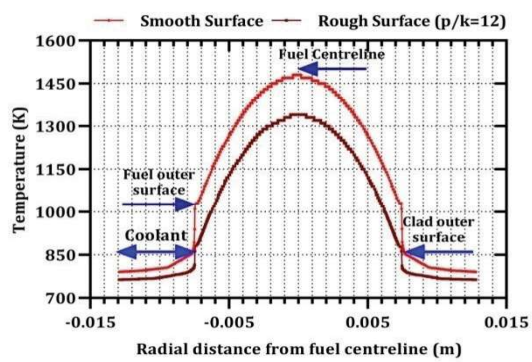

(g)

Fig. 5. Comaprision of temperature distribution from fuel to coolant for sommth and rough cladding surface (a) $p/k=6$ (b) $p/k=7$ (c) $p/k=8$ (d) $p/k=9$ (e) $p/k=10$ (f) $p/k=11$ (g) $p/k=12$

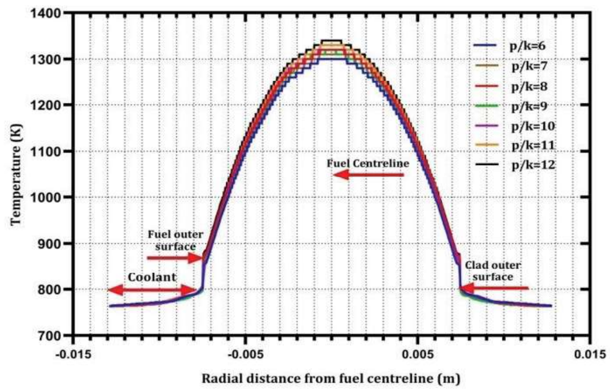

Fig. 6. Comparison of temperature distribution for different p/k values

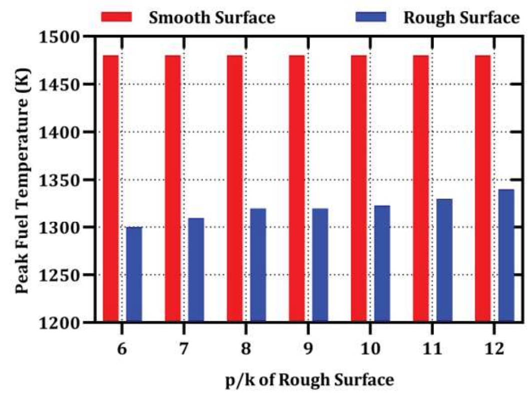

Fig. 7. Comparison of peak fuel temperature

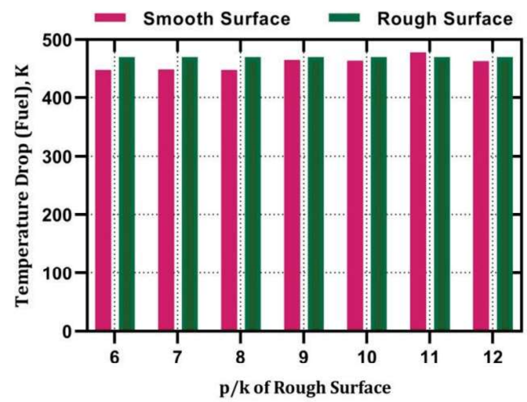

Fig. 8. Comparison of temperature drop across the fuel

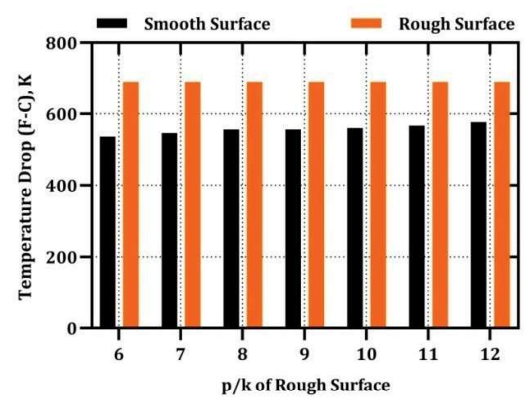

Fig. 9. Comparison of temperature drop from fuel to coolant

The area of the heated surface has a dominant impact on the heat transfer rate that controls the fuel temperature. Figure 4 shows how the surface area of the heated fuel cladding varies with the pitch to height ratio (p/k) of the square transverse ribs. Obviously, the lower p/k values allow more ribs on the cladding surface and hence the higher surface area. The temperature distribution from fuel to coolant for the smooth and rough cladding surface is shown in Fig 5. For the better visualization, rough surfaces are compared in Fig. 6. The nuclear fuel of AGR is a solid cylindrical rod and it is evident that the temperature profile in this geometry looks like a bell-shaped curve. The variation is observed in this study. For both types of cladding surfaces (smooth and rough surfaces), the maximum temperature is found at the center of the fuel, then temperature decreases from fuel to coolant as like as a bell-shaped curve. It is seen that the fuel temperature reduces to a substantial amount due to surface roughness. This lower fuel temperature results from the higher heat transfer rate which prevents the fuel temperature escalation. The lower fuel temperature reduces the fuel swelling which minimizes the fuel pellet cladding interaction and fuel failure. In addition to that higher thermal conductivity of UO_2 at low temperature promotes heat transfer rate. Figure 7 shows the peak fuel temperature which is found at the centre of the fuel. A significant reduction in the fuel centerline temperature for the rough surface is observed. The highest value is found for the smooth surface (1440K) whereas the lowest value is 1300K for rough cladding surface with $p/k = 6$. The peak fuel temperature shows a decreasing pattern with increasing surface roughness. These lower values increase the operating safety margin of the reactor and ensure enhanced safety of the plant. Figure 8 shows the temperature drop across the fuel pellet. A higher drop is observed for the fuel with a rough cladding surface. No well-defined pattern is found for different surface roughness. The temperature drop from fuel to the coolant is shown in Fig. 9. Lower values are seen for the rough cladding surface. Therefore, heat loss can be minimized by this technique.

4. Conclusion

The bell-shaped radial temperature profile was generated for both smooth and rib roughed cladding and compared. The fuel rod with a rough cladding surface has a slightly flatter temperature distribution curve with a lower peak fuel temperature. The higher heat transfer rate due to the higher surface area of rib roughed cladding results in a lower fuel temperature within the fuel. The maximum fuel temperature shows a decreasing pattern with decreasing pitch-to-height ratio. A higher range of fuel to coolant temperature is observed for the fuel rod with the smooth clad surface while surface roughness in the cladding reduces this range. Lower fuel temperature will reduce the cracking in the oxide ceramic fuel and minimize the fuel failure risk.

References

1 N. E. Todreas, and M. S. Kazimi, "Nuclear Systems: Volume 1", London: Taylor & Francis. Chapter 2, 1990,

2 A.E. Bergles, V. Nirmalan, G.H. Junkhan, R.L. Webb, "Bibliography on Augmentation of Convective Heat and Mass Transfer—II", United States Department of Energy, 1983

3 J. R Lamarsh, A.J. Baratta, "Introduction to Nuclear Engineering" Third ed, New Jersey: Prentice-Hall, 2001, Chapter 8.

4 A. Keshmiri, "Three-dimensional simulation of a simplified advanced gas-cooled reactor fuel element", Nuclear Engineering, and Design, vol. 241, pp. 4122– 4135, 2011.

5 A. Keshmiri, and J. Gotts, "Thermal-hydraulic analysis of four geometrical design parameters in rib-roughened channels", Numerical Heat Transfer, Part A, pp 305–327, 2011.

6 A. Ooi, G. Iaccarino, P.A. Durbin, M. Behnia, "Reynolds averaged simulation of flow and heat transfer in ribbed ducts", International Journal of Heat and Fluid Flow, vol. 23, pp. 750–757, 2002.

7 W. F Cope, "The Friction and Heat Transmission Coefficients of Rough Pipes" Froc. Inst. Mechanical Engineers, pp. 99–105, 1941.

8 T. S. Ravigururajan, "General correlations for pressure drop and heat transfer for single-phase turbulent flows in ribbed tubes" Iowa State University, pp. 18–19, 1986.

9 E. Nonbel, "Description of the Advanced Gas-Cooled Type of Reactor (AGR)" Nord. Nucl. Saf. Res. NKS/RAK2 (96) TR-C2.,1996.

10 S. G. Popov, J. J. Carbajo, V. K. Ivanov, G. L. Yoder, "Thermophysical Properties of MOX and UO_2 Fuels Including the Effects of Irradiation". J. Russ. Res. Cent. Oak Ridge Natl. Lab. pp. 9–24. 2000.

11 C. S. Kim, "Thermophysical Properties of Stainless Steels", Argonne Natl. Lab. pp. 2–13. 1975.

12 M. M. Rathore, "Thermal Engineering", pp. 1067–1116, 2010.

13 Ansys, Release 17.0, Help System, Mechanical APDL Documentation, ANSYS, Inc.

14 S. Zainal, C. Tan, C. J. Sian, and T. J. Siang, "Ansys simulation for Ag / HEG Hybrid Nanofluid in Turbulent Circular Pipe", vol. 23, no. 1, pp. 20–35, 2016.

15 J. J. Duderstadt, and L. J. Hamilton, "Nuclear Reactor Analysis", New York: Wiley, Chapter 12. 1976.

16 S. G. Popov, J.J. Carbajo, V.K. Ivanov and G.L. Yoder' "Thermophysical Properties of MOX and UO_2 Fuels Including the Effects of Irradiation", Engineering Technology Division, Fissile Materials Deposition Program, Oak Ridge National Laboratory. ORNL/TM/-2000/351, 2000.

17 F. I. Farha and M.H. Sahadath, "Modeling and Simulation of Radial Temperature, Thermal Heat Flux, and Thermal Gradient Distribution in Solid and Annular Nuclear Fuel Element of Uranium Dioxide", DUJASE, vol. 6, no.1, pp. 1-8, 2021.

18 F. I. Farha, M. H. Sahadath, S. H. Nishat, "Thermal-hydraulic analysis of UO_2 and MOX fuel considering different cladding materials at various burnup levels in pressurized water reactor". Heat Transfer, Wiley LLC, pp.1-17. 2021.